Dihydrodipicolinate Synthase from *Escherichia coli*: pH Dependent Changes in the Kinetic Mechanism and Kinetic Mechanism of Allosteric Inhibition by L-Lysine†

William E. Karsten

Department Biochemistry and Molecular Biology, University of North Texas Health Science Center, 3500 Camp Bowie Boulevard, Fort Worth, Texas 76107

Received September 9, 1996⊗

ABSTRACT: Dihydrodipicolinate synthase (DHDPS) catalyzes the formation of dihydrodipicolinate from pyruvate and L-aspartate β-semialdehyde (ASA). A parallel initial velocity pattern that displays competitive substrate inhibition by ASA and dead-end inhibition patterns obtained at pH 8 are consistent with a ping pong kinetic mechanism for DHDPS. The results suggest that pyruvate binds to free enzyme with subsequent formation of a Schiff base with an enzymic lysine residue followed by binding of ASA to the F enzyme form to initiate the second half-reaction. At low pH (5.7) the initial velocity and dead-end inhibition patterns are consistent with a sequential steady state ordered kinetic mechanism with pyruvate binding to enzyme prior to ASA. The irreversible step in the reaction, leading to the ping pong kinetic mechanism at high pH, is proposed to be loss of a proton from the methyl group of pyruvate in Schiff base with enzyme to form an enamine intermediate. Consistent with this proposal is the change to a sequential steady state ordered kinetic mechanism at low pH at or below the pK of the enamine intermediate. L-Lysine is an allosteric inhibitor of the DHDPS reaction that causes partial inhibition (~90%) at saturating concentrations. Inhibition patterns for L-lysine vs pyruvate and ASA suggest that lysine binds to the F enzyme form at pH 8 with a K_i value of about 0.3 mM. An examination of the effects of different L-lysine concentrations on the kinetic parameters $V/K_{pyruvate}$, V/K_{ASA}, and V indicate that L-lysine decreases only the values of V/K_{ASA} and V_{max}, which is consistent with the inhibitory effects of lysine manifested on the second half-reaction. In contrast at low pH the data suggest L-lysine binds to free enzyme with an inhibition constant of about 5 mM.

Dihydrodipicolinate synthase (EC 4.2.1.52) catalyzes the formation of 2,3-dihydrodipicolinate from pyruvate and L-aspartate β-semialdehyde. DHDPS[1] catalyzes the first step specific to the biosynthesis of *meso*-diaminopimelate and L-lysine in *Escherichia coli* and other bacteria. The immediate precursor of L-lysine is *meso*-diaminopimelate which is a component of the bacterial cell wall and is required for spore cortex formation in sporulating bacteria (Yamakura et al., 1974). DHDPS is also present in the chloroplasts of higher plants where it catalyzes the first reaction unique to the biosynthesis of L-lysine. Dihydrodipicolinate, the product of the DHDPS reaction, is a precursor of dipicolinate which is found in bacterial spores. The *E. coli dapA* gene which encodes DHDPS has been cloned and sequenced (Richaud et al., 1984). Based on the nucleotide sequence, a subunit molecular weight of 31 372 has been deduced for the apparently homotetrameric DHDPS. Unlike six of the nine enzymes present in the lysine biosynthetic pathway, the intracellular levels of DHDPS are not regulated at the genetic level by L-lysine (Bouvier et al., 1984). The *E. coli* enzyme shares overall about 55% similarity and 40% identity with the enzymes from wheat (Kaneko et al. 1990), maize (Frisch et al. 1991), and *Corynebacterium glutamicum* (Bonnassie et al., 1990) including several regions of higher homology. The enzymes studied to data from higher plants and sporulating bacteria are reported to be feedback inhibited by L-lysine in an allosteric fashion with the plant enzymes more sensitive to L-lysine levels than the *E. coli* enzyme (Yugari & Gilvarg, 1962; Cheshire & Miflin, 1975; Wallsgrove & Mazelis, 1981; Kumpaisal et al., 1987; Frisch et al., 1991; Laber et al., 1992). In contrast, the enzymes from sporulating *Bacillus subtilis* and *Bacillus licheniformis* have been reported to be insensitive to L-lysine inhibition (Stahly, 1969; Yamakura et al., 1974).

Pyruvate has been shown to form a Schiff base with an enzymic lysine residue (Shedlarski & Gilvarg, 1970). Later work by Laber et al. (1992) indicated that lysine 161 in the protein amino acid sequence forms the Schiff base with pyruvate. Additional evidence for formation of a covalent intermediate between pyruvate and enzyme comes from the electrospray mass spectrometry work on DHDPS conducted by Borthwick et al. (1995). The crystal structure of the *E. coli* enzyme has been solved at 2.5 Å resolution. Lysine 161 is located within a 30 × 10 Å cleft in the enzyme monomer that presumably comprises the active site (Mirwaldt et al. 1995).

Solely on the basis of the observation of initial velocity patterns that appear parallel, a ping pong kinetic mechanism has been proposed for the DHDPS from wheat (Kumpaisal et al., 1987), pea (Dereppe et al., 1992), and *E. coli* (Laber et al., 1992). Working with the enzyme from maize, Frisch et al. (1991) concluded that their data were consistent with

† This work was supported by grant GM 36799 to P. F. Cook from the National Institutes of Health.

⊗ Abstract published in *Advance ACS Abstracts,* January 15, 1997.

[1] Abbreviations: AEC, *S*-(2-aminoethyl)-L-cysteine; ASA, L-aspartate β-semialdehyde; DHD, dihydrodipicolinate; DHDPR, dihydrodipicolinate reductase; DHDPS, dihydrodipicolinate synthase; Hepes, *N*-(2-hydroxyethyl)piperazine-*N*′-ethanesulfonic acid; Mes, 2-(*N*-morpholino)-ethanesulfonic acid; NADH, reduced nicotinamide adenine dinucleotide; NADPH, reduced nicotinamide adenine dinucleotide phosphate; PCR, polymerase chain reaction.

S0006-2960(96)02264-7 CCC: $14.00

a ping pong mechanism, but due to certain kinetic complexities in the data this conclusion was considered uncertain. In contrast, working with the spinach leaf enzyme, Wallsgrove and Mazelis (1981) reported that the same apparent K_m value for ASA is obtained at different pyruvate concentrations, an observation which is consistent with a sequential kinetic mechanism. Substrate inhibition by ASA has been reported for the enzymes from various plant sources (Mazelis et al., 1977; Wallsgrove & Mazelis, 1981; Kumpaisal et al., 1987; Frisch et al., 1991) and *Bacillus licheniformis* (Stahly, 1969) but not the *E. coli* DHDPS (Laber et al., 1992) or the enzyme from pea (Dereppe et al., 1992). The substrate inhibition by ASA has been attributed to inhibition by sodium or potassium ions present in ASA solutions resulting from addition of NaOH or KOH to neutralize acidic ASA stock solutions prior to use in enzyme assays (Kumpaisal et al., 1989). Later work by Frisch et al. (1991) suggested the inhibition by ASA is competitive vs pyruvate and additional studies ruled out the possibility of inhibition by sodium. Cooperative binding by pyruvate has been reported for the enzymes from some plant sources (Wallsgrove & Mazelis, 1981; Frisch, 1991) but not others (Kumpaisal et al., 1987). An initial kinetic characterization of the *B. licheniformis* enzyme suggested cooperative pyruvate binding (Stahly, 1969), but later work by Halling and Stahly (1976), when care was taken to carefully measure initial velocities, showed no cooperativity in pyruvate binding.

Inhibition of the DHDPS reaction by L-lysine has been demonstrated for the enzyme from plants (Mazelis et al., 1977; Wallsgrove & Mazelis, 1981; Kumpaisal et al., 1987; Frisch et al., 1991; Dereppe et al., 1992) and *E. coli* (Yugari & Gilvarg, 1962) and attributed to allosteric feedback inhibition. The early work by Yugari and Gilvarg (1962) with the *E. coli* enzyme suggested that L-lysine is a competitive inhibitor vs ASA. Also with the *E. coli* enzyme, Laber et al. (1992) reported that at high L-lysine concentrations the inhibition by L-lysine is partial. The mechanism of L-lysine inhibition of the DHDPS from wheat has been investigated to some extent by Kumpaisal et al. (1987). These workers reported that L-lysine is a noncompetitive inhibitor vs pyruvate and a competitive inhibitor vs ASA. On the basis of these inhibition patterns it was suggested that L-lysine binds to the F enzyme form at the ASA binding site via the alanyl moiety of L-lysine. However, it is difficult to rationalize the proposal that L-lysine competes with ASA at its binding site with the observation that L-lysine causes only partial inhibition of the DHDPS reaction (Kumpaisal et al., 1987; Laber et al. 1992). Working with the pea enzyme, Dereppe et al. (1992) reported that L-lysine and L-α-(2-aminoethoxyvinylglycine) are noncompetitive inhibitors vs ASA, but another lysine analog, *S*-(2-aminoethyl)-L-cysteine, is competitive vs ASA. In contrast, the kinetic data of Frisch et al. (1991) working with the enzyme from maize led these workers to suggest that L-lysine is a competitive inhibitor vs pyruvate and a mixed-type inhibitor vs ASA. The kinetic mechanism of L-lysine inhibition of the *E. coli* enzyme has not been studied.

The aforementioned kinetic studies of DHDPS from different sources has led to a variety of results regarding the kinetic mechanism and the nature of allosteric inhibition and prompted the present investigation. In the present work the kinetic mechanism of the *E. coli* enzyme is investigated using initial velocity and dead-end inhibition studies at both high and low pH. The kinetics of inhibition by L-lysine is examined at high and low pH by dead-end inhibition studies and the method developed by Cook (1982) to examine the mechanism of enzyme inhibition by allosteric effectors.

MATERIALS AND METHODS

Materials. The ASA used in these studies was synthesized according to the procedure of Black and Wright (1955) that involves the essentially quantitative synthesis of ASA by ozonolysis of L-allylglycine followed by purification on a Dowex 50 column. Concentrations of stock ASA solutions were determined by the method of Karsten and Viola (1992). The restriction endonucleases and T4 DNA ligase were purchased from Promega and the IPTG, X-gal, and triethanolamine were from Fisher. Ampli-*Taq* was purchased from Perkin-Elmer Cetus, the pTZ19R vector was from Pharmacia, and the T4 polynucleotide kinase was purchased from United States Biochemical Corporation. Hepes and Mes buffers were purchased from Research Organics. Pyruvate, L-lysine, NADPH, NADH, and all substrate analogs were purchased from Sigma and were used without further purification. The Blue-A agarose matrix gel was purchased from Amicon. All other reagents were purchased commercially and were of the highest quality available.

Cloning of the dapA and dapB Genes. In order to provide large quantities of DHDPS and DHDPR, a PCR-based method was used to clone the *dapA* and *dapB* genes from *E. coli*. Genomic DNA was isolated from *E. coli* (Sambrook et al., 1989). For cloning of the genes two primers were used, one upstream from the gene of interest at the beginning of the published sequence for the gene (Bouvier et al., 1984; Richaud et al., 1986), and a second primer for the complementary strand at the end of the gene overlapping the translation stop codon. The polymerase chain reaction was used to amplify the target sequence containing the gene. For cloning the *dapA* gene, the upstream PCR primer sequence was 5′-GGCAAGCTTCCAGGCGACTGT CTTCAA-3′ and the downstream primer sequence was 5′-ACTGCAGCTT-TACAGCAAAC CGGCAT-3′. Cloning of the *dapB* gene was accomplished using an upstream oligonucleotide primer with the sequence 5′-AGGATCCTCGACTCATGCCTT-TCACTG-3′ and the downstream primer sequence 5′-CGAATTCGGTTACAAATTATTGAGATC-3′. Prior to performing the PCR reaction, the primers were phosphorylated using T4 polynucleotide kinase and the PCR reaction was carried out following the Ampli-*Taq* manufacturer's recommended conditions. The vector DNA was cleaved in the multiple cloning site with the restriction enzyme *Bam*HI and the resulting 5′ overhang was flushed with T4 DNA polymerase according to procedures outlined in Sambrook et al. (1989). The blunt-end ligation of PCR products to the pTZ19R vector DNA, transformation of *E. coli* (JM109), and blue−white colony screening were performed according to standard procedures (Sambrook et al., 1989). A screen for correct recombinant plasmids was performed by analysis of restriction enzyme products on agarose gels of plasmids isolated from cultures inoculated with white colonies. One of the isolated plasmids (pDHDPS) that likely contained the *dapA* gene based on the initial screening procedures was subjected to dideoxy DNA sequencing to confirm the presence of the *dapA* gene.

Purification of DHDPS. Growth of *E. coli* strain JM109 containing pDHDPS was started in YT media (Sambrook et

al., 1989) and grown to late-log phase at 37 °C with shaking. A total of 3.6 L of M9 minimal media (Sambrook et al., 1989) was inoculated with 1/10 volume of the YT culture and incubated at 37 °C with shaking in an orbital shaker for seven hours. The cells were harvested by centrifuging at 15000*g* for 20 min. The cells were suspended in 100 mL of buffer A (10 mM triethanolamine, pH 7.5, 10 mM β-mercaptoethanol) and disrupted by sonic oscillation. The cell debris was pelleted by centrifugation at 15000*g* for 20 min. An 11% (w/v) streptomycin sulfate solution was added to the resulting supernatant solution, 9 mL per 100 mL of supernatant solution, with stirring at 4 °C. After an additional 15 min of stirring the solution was centrifuged for 25 min at 15000*g*. Solid pyruvate was added to the supernatant to a final concentration of 1.5 mM. The enzyme solution was adjusted to pH 5.5 with 1 M acetic acid and heated to 55 °C for 2 min. The solution was transferred to an ice bath and adjusted to pH 7.0 by the addition of 1 M KOH. The solution was centrifuged for 30 min at 15000*g*. Solid ammonium sulfate was added to the supernatant solution to 80% saturation with stirring at 4 °C. After at least 30 min the enzyme solution was centrifuged at 15000*g* for 30 min. The precipitated protein was dissolved in 20 mL of buffer A and dialyzed vs 2 × 500 mL of the same buffer.

The dialyzed enzyme solution was loaded at room temperature onto a DEAE-cellulose column (2.5 × 30 cm) preequilibrated with buffer A and washed with at least 5 bed volumes of buffer A until the absorbance at 280 nm of the column effluent equaled zero. The enzyme was then eluted with a linear sodium chloride gradient (0−500 mM) with a total volume of 800 mL. Fractions with the highest specific enzyme activities were pooled and ammonium sulfate was added to 80% saturation. After overnight storage at 4 °C, the enzyme solution was centrifuged at 15000*g* for 30 min. The precipitated protein was dissolved in a minimal volume of buffer A and loaded onto a phenyl-Sepharose column (2.5 × 12 cm) preequilibrated with buffer A containing 2 M ammonium sulfate. The column was washed with >4 bed volumes of buffer A containing 1 M ammonium sulfate and the enzyme was subsequently eluted with a linear ammonium sulfate gradient (1−0 M) of 400 mL total volume. The fractions containing enzyme activity were pooled and the enzyme precipitated by the addition of ammonium sulfate to 80% saturation followed by centrifugation of the enzyme solution at 15000*g* for 30 min. The precipitated protein was dissolved in a minimal volume of buffer A, dialyzed vs buffer A, and stored in the same buffer at −20 °C. The enzyme is stable under these storage conditions for at least 6 months. The purification procedure is similar to a method developed by Laber et al. (1992).

Purification of DHDPR. *E. coli* strain JM109 with the *dapB* containing plasmid was grown in 3.6 L of YT media to late-log phase, and the cells were harvested as in the DHDPS enzyme purification procedure. A streptomycin sulfate step was performed according to the above procedure for the DHDPS preparation followed by an ammonium sulfate step according to the method of Farkas and Gilvarg (1970). The resulting enzyme solution was applied to a DEAE-cellulose column (2.5 × 18 cm) preequilibrated with buffer A. The column was washed with buffer A containing 100 mM NaCl and eluted with a linear NaCl gradient (100−600 mM) with a total volume of 600 mL. The active fractions were pooled and the protein was precipitated by the addition of ammonium sulfate to 80% saturation. After centrifugation at 15000*g* for 30 min, the protein pellet was dissolved in a minimal volume of buffer containing 50 mM Hepes, pH 7.0, and 10 mM β-mercaptoethanol (buffer B) and dialyzed vs the same buffer. The enzyme solution was loaded onto a Blue A agarose column (2.5 × 15 cm) preequilibrated with buffer B. After washing the column with buffer B containing 500 mM NaCl until the A_{280} of the column effluent was equal to zero, the enzyme was eluted with a linear NaCl gradient (0.5−1 M) with a total volume of 500 mL. The fractions containing enzyme activity were pooled and concentrated by the addition of ammonium sulfate according to the above procedure. The resulting enzyme is stored in buffer B at −20 °C and is stable under these storage conditions for at least one year. On the basis of visual inspection of SDS−polyacrylamide gels, the final enzyme preparation is greater than 90% pure containing a single minor contaminating protein band and a major band consistent with the monomer size of DHDPR. In order to follow the DHDPR purification procedure, DHDPR activity is assayed at 25 °C in 1 mL cuvettes containing 100 mM Hepes, pH 7.0, 100 μM ASA, 100 μM pyruvate, 200 μM NADPH, and about 1 unit of DHDPS. After a 10 min incubation to form DHD, DHDPR is added and the reaction is monitored at 340 nm by following the disappearance of NADPH.

Initial Velocity Studies. Initial velocity data were collected on a Gilford 260 spectrophotometer equipped with thermospacers and connected to a circulating water bath to maintain a constant temperature of 25 °C. Assays were performed in 1 mL cuvettes. A typical assay contained 100 mM Hepes, pH 8.0, 0.2 mM NADPH or NADH, 15−25 μg of DHDPR, and varied concentrations of the substrates ASA and pyruvate. DHDPR was included in the assays as a coupling enzyme at sufficient quantities to give linear reaction progress curves in all cases. The progress of the reactions was monitored by following the reduction of dihydrodipicolinate by NAD(P)H at 340 nm ($\epsilon_{340} = 6220\ M^{-1}\ cm^{-1}$) as catalyzed by DHDPR. For inhibition studies, assays contained the same components as for the initial velocity studies with one substrate maintained at a fixed concentration near its K_m value and the other substrate varied at different inhibitor concentrations. Dipicolinate was found to inhibit the coupling enzyme DHDPR, consequently it was necessary to include up to ten times the levels of DHDPR in assays containing dipicolinate compared to typical assays. Initial velocity patterns were also obtained at pH 8 in the presence of several different fixed concentrations of lysine. Initial velocity and dead-end inhibition patterns were also obtained at pH 5.7 and these assays contained 100 mM Mes, pH 5.7, 0.2 mM NADH, 25 μg of DHDPR, and varied concentrations of ASA and pyruvate. All substrates and enzymes are stable over the time course of the reaction. The measured initial rates are typically reproducible to within about 10%, but are somewhat less reproducible at very low substrate concentrations where the linear region of the progress curve is short.

Data Processing. Data were fitted to the appropriate rate equations using BASIC versions of the computer programs developed by Cleland (1979). To determine the equation which best fit the data a comparison of SIGMA values and the standard errors associated with the calculated values of the kinetic constants was made with the lowest values determining the chosen fit. Initial velocity data obtained at

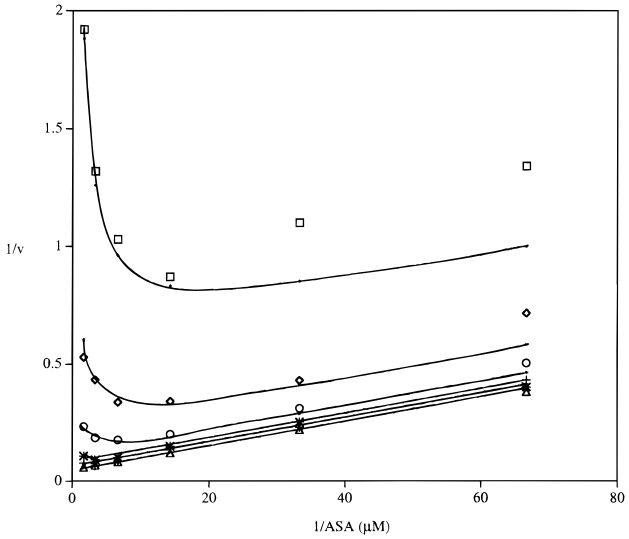

FIGURE 1: Initial velocity pattern at pH 8. Assays done as described in Methods with pyruvate concentrations as (□) 0.015, (◇) 0.050, (○) 0.150, (asterisks) 0.500, (+) 1.5, (△) 5 mM, and ASA concentrations varied from 0.015 to 0.6 mM. Data points are experimental and lines were generated from a fit using eq 1.

pH 8 in the absence and presence of L-lysine were fitted using eq 1 or 2, while data obtained at pH 5.7 was fitted using eq 3. Dead-end inhibition data were fitted to eqs 4−6.

$$v = VAB/(K_aB[1 + B/K_i] + K_bA[1 + A/K_i] + AB) \quad (1)$$

$$v = VAB/(K_aB + K_bA + AB) \quad (2)$$

$$v = VAB/(K_{ia}K_b + K_aB + K_bA + AB) \quad (3)$$

$$v = VA/(K_a[1 + I/K_{is}] + A) \quad (4)$$

$$v = VA/(K_a + A[1 + I/K_{ii}]) \quad (5)$$

$$v = VA/(K_a[1 + I/K_{is}] + A[1 + I/K_{ii}]) \quad (6)$$

In eqs 1−6, v is the initial velocity, V is the maximum velocity, A and B are the substrate concentrations, K_{ia} is the dissociation constant for A, I is the inhibitor concentration, and K_{is} and K_{ii} are the slope and intercept inhibition constants, respectively.

RESULTS

Purification of DHDPS. Based on SDS−polyacrylamide gels, about 10% of the total protein in crude extracts derived from *E. coli* JM109 containing pDHDPS is DHDPS, which is more than 100 times the enzyme levels observed in non-plasmid containing cells. This estimate in enzyme levels for pDHDPS containing *E. coli* is consistent with the approximately 10-fold purification afforded by the enzyme purification procedure. Little enzyme activity is lost up to the final phenyl-Sepharose column chromatography step. The overall yield is 60% and the final enzyme preparation is >90% pure on the basis of visual inspection of SDS−polyacrylamide gels.

Initial Velocity and Dead-End Inhibition Studies. A parallel initial velocity pattern obtained at pH 8 showing competitive substrate inhibition by ASA is presented in Figure 1. For the plant enzymes the reported $K_{I,ASA}$ is about 5 mM while the value for the *E. coli* enzyme is about 0.3 mM. A similar initial velocity pattern is also obtained at pH 7 (data not shown). A fit of the data to eq 1 yields the kinetic parameters listed in Table 1. Data obtained from inhibition patterns are presented in Table 2. β-Fluoropyruvate is a competitive inhibitor vs pyruvate and a noncompetitive inhibitor vs ASA. The other pyruvate analogs tested are competitive inhibitors vs pyruvate and uncompetitive inhibitors vs ASA. Succinic semialdehyde is a competitive inhibitor vs ASA and an uncompetitive inhibitor vs pyruvate. Dipicolinate is a competitive inhibitor vs pyruvate and an uncompetitive inhibitor vs ASA. Inhibition patterns were also obtained vs both substrates with the allosteric inhibitors L-lysine and AEC. L-Lysine and AEC are uncompetitive inhibitors vs pyruvate and the inhibition data vs ASA are fit best to the equation for noncompetitive inhibition. The inhibition constants for AEC are about one order of magnitude greater than the corresponding values for L-lysine. Most of the substrate analog inhibition constants are in the range 50−700 μM with the exception of dipicolinate which has an inhibition constant of about 10 mM.

Table 1: Kinetic Parameters for DHDPS[a]

parameter	pH 8[b]	pH 5.7[c]
V/E_t	$188 \pm 7\ s^{-1}$	$39 \pm 3\ s^{-1}$
$V/K_{pyruvate}/E_t$	$(9.7 \pm 1.7) \times 10^5\ M^{-1}\ s^{-1}$	$(2.4 \pm 0.6) \times 10^6\ M^{-1}\ s^{-1}$
$K_{pyruvate}$	$194 \pm 33\ \mu M$	$16 \pm 4\ \mu M$
$V/K_{ASA}/E_t$	$(1.5 \pm 0.1) \times 10^6\ M^{-1}\ s^{-1}$	$(8.5 \pm 1.5) \times 10^5\ M^{-1}\ s^{-1}$
K_{ASA}	$124 \pm 11\ \mu M$	$46 \pm 8\ \mu M$
K_I	$270 \pm 80\ \mu M$	

[a] Protein concentrations determined by the method of Bradford (1976) usng bovine serum albumin as protein standard. The molar concentrations of DHDPS used in the calculation of the values in the table are based on a molecular weight of 31 372 for the enzyme monomer. [b] Values determined at pH 8.0 with 100 mM Hepes buffer from a fit of the initial velocity data to eq 1. [c] Values determined at pH 5.7 with 100 mM Mes buffer from a fit of the initial velocity data to eq 3.

An initial velocity pattern obtained at pH 5.7 is presented in Figure 2. In contrast to the parallel pattern seen at pH 8, the initial velocity pattern obtained at low pH is of the intersecting type and no substrate inhibition by ASA observed under the assay conditions employed. The initial velocity data were fit using eq 3 to yield the kinetic parameters shown in Table 1. The data obtained from the dead-end inhibition patterns at pH 5.7 are presented in Table 2. Similar to what is observed at high pH each analog is a competitive inhibitor vs their respective substrate. Succinic semialdehyde is an uncompetitive inhibitor vs pyruvate, but unlike at high pH, the pyruvate analogs are noncompetitive inhibitors vs ASA.

Inhibition by Lysine. A Dixon plot of DHDPS inhibition by L-lysine or AEC (data not shown) displays cooperative inhibition by both inhibitors. A Hill plot of the L-lysine data results in a Hill coefficient of about 1.4 and an $I_{0.5}$ value of about 0.4 mM. The same $I_{0.5}$ value is obtained at different substrate concentrations. Dixon plots asymptotically approach a finite rate at saturating L-lysine or AEC concentrations leading to about 90% and 75% inhibition, respectively, consistent with the report by Laber et al. (1992) of partial L-lysine inhibition (~80%) at high L-lysine concentrations. Similar cooperative inhibition by L-lysine, AEC, and several other L-lysine analogs has been reported for the DHDPS from wheat (Kumpaisal et al., 1987). The L-lysine inhibition patterns vs pyruvate and ASA are shown in Figure 3.

Table 2: Dead-End Inhibition Patterns for DHDPS[a]

fixed substrate	varied substrate	inhibitor	pattern	K_{is} (mM)	K_{ii} (mM)
			Patterns at pH 8[b]		
pyruvate analogs					
ASA	pyruvate	3-fluoropyruvate	competitive	0.22 ± 0.02	−
pyruvate	ASA	3-fluoropyruvate	noncompetitive	2.0 ± 0.6	0.7 ± 0.1 (0.2)[c]
ASA	pyruvate	2-ketobutyrate	competitive	0.83 ± 0.06	−
pyruvate	ASA	2-ketobutyrate	uncompetitive	−	1.3 ± 0.1 (0.4)
ASA	pyruvate	2-ketovalerate	competitive	0.7 ± 0.2	−
pyruvate	ASA	2-ketovalerate	uncompetitive	−	1.6 ± 0.2 (0.5)
ASA	pyruvate	glyoxalate	competitive	0.016 ± 0.002	−
pyruvate	ASA	glyoxalate	uncompetitive	−	0.028 ± 0.004 (0.010)
ASA analog					
ASA	pyruvate	succinic semialdehyde	uncompetitive	−	0.07 ± 0.005 (0.03)
pyruvate	ASA	succinic semialdehyde	competitive	0.044 ± 0.007	−
DHD analog					
ASA	pyruvate	dipicolinate	competitive	11 ± 2	−
pyruvate	ASA	dipicolinate	uncompetitive	−	18 ± 2 (6)
lysine analogs					
ASA	pyruvate	L-lysine	uncompetitive	−	0.29 ± 0.04
pyruvate	ASA	L-lysine	noncompetitive	0.2 ± 0.1	0.4 ± 0.1
ASA	pyuvate	AEC	uncompetitive	−	1.9 ± 0.3
pyruvate	ASA	AEC	noncompetitive	2.4 ± 1.6	4.7 ± 2.3
			Patterns at pH 5.7[d]		
pyruvate analogs					
ASA	pyruvate	glyoxylate	competitive	0.024 ± 0.004	
pyruvate	ASA	glyoxylate	noncompetitive	0.160 ± 0.04	0.21 ± 0.03
ASA	pyruvate	2-ketobutyrate	competitive	0.65 ± 0.05	
pyruvate	ASA	2-ketobutyrate	noncompetitive	3.8 ± 2.5	1.8 ± 0.3
ASA analog					
ASA	pyruvate	succinic semialdehyde	uncompetitive		0.067 ± 0.005
pyruvate	ASA	succinic semialdehyde	competitive	0.037 ± 0.009	
L-lysine					
ASA	pyruvate	L-lysine	noncompetitive	4.7 ± 2.8	4.6 ± 0.8
pyruvate	ASA	L-lysine	noncompetitive	3.1 ± 1.4	5.2 ± 1.5

[a] Most inhibition patterns were obtained twice with qualitatively and quantitatively similar results. [b] The data were obtained at pH 8.0 with 100 mM Hepes buffer as described in Methods. [c] Values in parentheses are true K_i values calculated from $K_i = K_{i,app}/(1 + S/K_m)$ where S is the fixed substrate concentration. [d] The data were obtained at pH 5.7 with 100 mM Mes buffer as described in Methods.

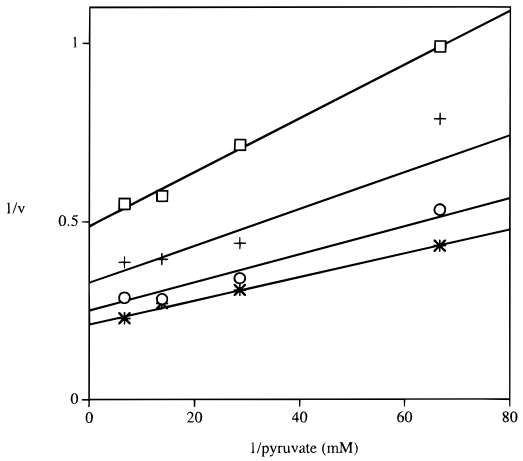

FIGURE 2: Initial velocity pattern at pH 5.7. Assays done as described in Methods with pyruvate varied from 0.015 to 0.15 mM and ASA concentrations (□) 0.025, (+) 0.05, (○) 0.1, and (asterisks) 0.2 mM. Data points are experimental and lines were generated from a fit using eq 3.

In order to examine the mechanism of L-lysine inhibition after the method of Cook (1982), initial velocity patterns were obtained at pH 8 in the absence and presence of different L-lysine concentrations. The effects of L-lysine on the kinetic parameters are presented in Table 3. In all cases parallel initial velocities patterns are obtained. Compared to the values determined in the absence of L-lysine, at increasing L-lysine concentrations V and V/K_{ASA} progressively decrease at increasing L-lysine levels to a limit approximately 10-fold lower than in the absence of L-lysine. In contrast, $V/K_{pyruvate}$ remains unchanged at all L-lysine concentrations. Dissociation constants determined from the secondary replots give the values for L-lysine of 0.57 ± 0.42 mM from the effects on V and 0.57 ± 0.13 mM from the L-lysine effects on V/K_{ASA}, similar to the values of $K_{i,lysine}$ determined from the L-lysine inhibition patterns presented in Table 2.

At pH 5.7 cooperative inhibition by L-lysine is observed (data not shown) with a Hill coefficient of about 1.8 and a maximum inhibition at saturating L-lysine of about 85% similar to that seen at high pH. However, the $I_{0.5}$ value is about 8 mM compared to 0.4 mM at pH 8. In contrast to what is seen at high pH, L-lysine inhibition patterns vs pyruvate or ASA both display a slope and intercept effect. In order to estimate inhibition constants the patterns were fit using eq 6 and the data are shown in Table 2. The effects of increasing L-lysine concentrations on the kinetic parameters obtained at pH 5.7 are presented in Table 4 and in all cases intersecting initial velocity patterns are observed. At low pH all three kinetic parameters, $V/K_{pyruvate}$, V/K_{ASA}, and V, decrease progressively with increasing L-lysine concentrations. The secondary replot of 1/L-lysine vs $V/K_{pyruvate}$ yields dissociation constants of 4.7 ± 2.5 mM similar to the L-lysine K_i values reported in Table 2. The secondary replot of the V data is nonlinear and provides an estimated L-lysine dissociation constant to central complexes of 3.6 ± 1.8 mM. The secondary replot of the V/K_{ASA} data passes near the

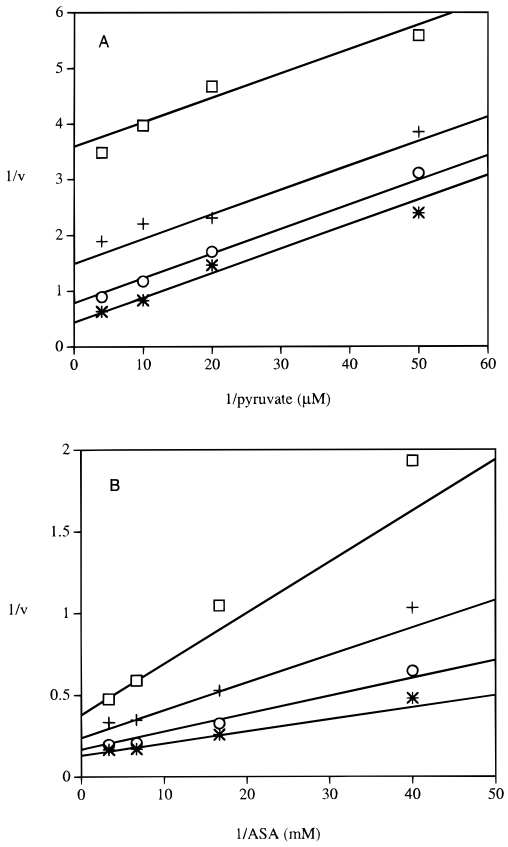

FIGURE 3: Lysine inhibition patterns vs pyruvate (A) and ASA (B) at pH 8. (A) Assays contained 100 mM Hepes, pH 8, varied concentrations of pyruvate (50−500 μM) and L-lysine (asterisks) 0, (○) 0.1, (+) 0.3, and (□) 0.9 mM. Data points are experimental and the lines are derived from a fit of the data using eq 5. (B) Assays contained 100 mM Hepes, pH 8, varied concentrations of ASA (30−300 μM) and L-lysine (asterisks) 0, (○) 0.1, (+) 0.3, and (□) 0.9 mM Data points are experimental and the lines are derived from a fit of the data using eq 6.

origin and yields a poorly defined dissociation constant of 12 ± 11 mM.

DISCUSSION

There are shortcomings to the assay methods previously used to measure DHDPS activity including lags in the reaction time courses and uncharacterized reaction products that do not allow acquisition of quantitative kinetic data. The problems with these assay methods have been discussed previously (Borthwick et al., 1995). The problems associated with the assay methods may account for the various contradictory reports regarding pyruvate cooperative binding kinetics, L-lysine inhibition patterns vs different substrates, and suggests the possibility of other artifactual results. An assay method for collecting reliable kinetic data on DHDPS was clearly needed and the coupled enzyme assay method using DHDPR first described by Shedlarski and Gilvarg (1965) was considered a good candidate. Consequently, the *dapB* gene from *E. coli* was cloned to provide an ample supply of DHDPR and the enzyme purified. The coupled DHDPR assay method employed in the present studies results in linear reaction progress curves in all cases and allows initial velocities to be measured accurately. Since the reaction is followed by monitoring the oxidation of NAD(P)H, quantitative enzyme rate data are available for DHDPS.

Kinetic Mechanism of DHDPS. A ping pong kinetic mechanism has been proposed for DHDPS based solely on the observation of initial velocity patterns that appear parallel (Kumpaisal et al., 1987; Derepe et al., 1992; Laber et al., 1992). Although suggestive of a ping pong kinetic mechanism, an initial velocity pattern that yields a family of apparently parallel lines is insufficient evidence to base assignment of a ping pong mechanism since a sequential kinetic mechanism will display an initial velocity pattern that appears parallel if certain kinetic conditions apply (Segel, 1975; Cleland, 1977; Dixon & Webb, 1979). The assignment of a ping pong kinetic mechanism to DHDPS is all the more tenuous when the nature of the proposed sequence of substrate binding and product release steps is considered. It has been proposed that pyruvate binds to free enzyme followed by Schiff base formation and release of a water molecule prior to ASA binding to the F enzyme form (Kumpaisal et al., 1989; Laber et al., 1992). A ping pong kinetic mechanism requires that an irreversible step, typically first product release, be present between the binding of the first and second substrate. The presence of the first product, in this case 55.5 M H_2O, would be expected to lead to reversibility of the first half-reaction and an intersecting initial velocity pattern (Dixon & Webb, 1979). In consideration of the issues raised above, an investigation of the kinetic mechanism of DHDPS was undertaken.

The parallel initial velocity pattern obtained at pH 8 in this study is suggestive of a ping pong kinetic mechanism. ASA displays competitive substrate inhibition vs pyruvate which is diagnostic for a ping pong kinetic mechanism. A ping pong kinetic mechanism represents a symmetrical situation, so that if ASA binds to E to form a dead-end complex, increasing concentrations of pyruvate should eliminate inhibition by ASA. The substrate K_m values reported here for the *E. coli* enzyme are about an order of magnitude lower than have been reported for the enzymes from higher plants (Wallsgrove & Mazelis, 1981; Kumpaisal et al., 1987) and about 4-fold lower than those reported previously for the *E. coli* enzyme (Laber et al., 1992). The discrepancies between the values of the kinetic parameters reported here and those by Laber et al. (1992) may be due to the differences in the assay methods employed in the two studies. The K_{ASA} values reported here or in previous studies do not take into account that about 85% of the ASA aldehyde functional group is hydrated at pH 7.5 (Shames & Wedler, 1984). The aldehyde, rather than the hydrate is almost certainly the actual substrate. Consequently the true K_{ASA} values are considerably less than the reported values. A comparison, however, of the relative values is still valid.

In order to further investigate the kinetic mechanism dead-end inhibition patterns were obtained for the DHDPS reaction and were also found to be consistent with a ping pong mechanism. As expected for dead-end inhibitors in a ping pong kinetic mechanism in which there are two stable enzyme forms, E and F, substrate analogs are competitive inhibitors vs the substrate of which they are an analog and uncompetitive inhibitors vs the other substrate. Dipicolinate, an analog of dihydrodipicolinate, is an uncompetitive inhibitor vs ASA and a competitive inhibitor vs pyruvate indicating that dipicolinate binds to a different enzyme form than ASA and to the same enzyme form that binds pyruvate. One exception to the overall trend in the inhibition patterns is

Table 3: Kinetic Parameters for DHDPS Determined in the Presence of Different Lysine Concentrations at pH 8[a]

	lysine (mM)				
	0	0.07	0.2	0.6	5.0
V	8.7 ± 0.7[b]	7.3 ± 0.5	4.1 ± 0.2	1.2 ± 0.1	0.7 ± 0.07
$V/K_{pyruvate}$	51 ± 6	45 ± 4	44 ± 4	56 ± 14	64 ± 20
V/K_{ASA}	125 ± 14	98 ± 9	37 ± 2	22 ± 2	13 ± 1
$K_{pyruvate}$	0.17 ± 0.03	0.16 ± 0.02	0.09 ± 0.01	0.021 ± 0.006	0.010 ± 0.004
K_{ASA}	0.07 ± 0.01	0.07 ± 0.01	0.110 ± 0.009	0.053 ± 0.007	0.053 ± 0.009

[a] Assays conducted with 100 mM Hepes, pH 8.0, at 25 °C. [b] Units are nmol/min for V, min^{-1} for V/K, and mM for substrate K_m values. Kinetic parameters determined from a fit of the initial velocity data using eq 2.

Table 4: Kinetic Parameters for DHDPS Determined in the Presence of Different Lysine Concentrations at pH 5.7[a]

	lysine (mM)				
	0	1.5	3	6	15
V	10.5 ± 0.7[b]	8.6 ± 0.8	6.5 ± 0.4	4.8 ± 0.7	2.4 ± 0.3
$V/K_{pyruvate}$	660 ± 130	290 ± 66	192 ± 24	158 ± 30	66 ± 14
V/K_{ASA}	228 ± 52	178 ± 46	100 ± 10	53 ± 15	19 ± 3
$K_{pyruvate}$	0.016 ± 0.004	0.030 ± 0.009	0.034 ± 0.006	0.031 ± 0.016	0.04 ± 0.01
K_{ASA}	0.046 ± 0.008	0.05 ± 0.02	0.07 ± 0.01	0.09 ± 0.04	0.13 ± 0.03

[a] Data obtained with 100 mM Mes, pH 5.7, at 25 °C. [b] Units are nmol/min for V, min^{-1} for V/K, and mM for substrate K_m values. Values reported at 0 lysine concentration were normalized to the enzyme concentration used in assays contaning lysine. Kinetic parameters determined from a fit of the initial velocity data using eq 3.

Scheme 1

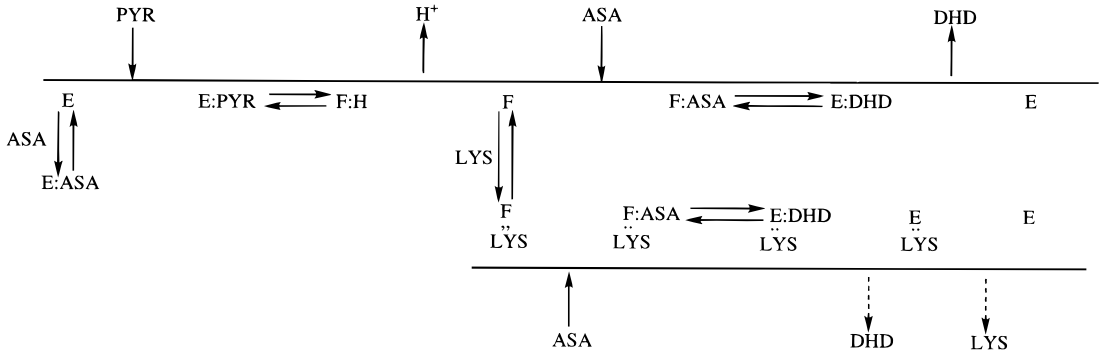

β-fluoropyruvate, which appears to be competitive vs pyruvate and noncompetitive vs ASA, probably the result of β-fluoropyruvate binding to both stable enzyme forms. The inhibition of DHDPS by β-fluoropyruvate reported here is in contrast to the report by Laber et al (1992) that β-fluoropyruvate is not an inhibitor of DHDPS. In a ping pong mechanism K_{ii} values may be corrected for the fixed substrate concentration to give true K_i values which should agree with the K_{is} value for that inhibitor vs its competing substrate and, as shown in Table 2, there is reasonable agreement in all cases. Overall the initial velocity and dead-end inhibition patterns are consistent with a ping pong kinetic mechanism in which pyruvate and DHD bind to free enzyme (E) and ASA binds to F, the other stable enzyme form. The kinetic mechanism, including substrate inhibition by ASA, is illustrated in the upper portion of Scheme 1.

A ping pong kinetic mechanism requires two stable enzyme forms and the presence of an irreversible step between binding of the two substrates which typically is release of the first product. In the case of DHDPS, formation of a Schiff base between pyruvate and an enzyme lysine residue will eliminate water. Can release of water in an aqueous assay environment constitute an irreversible step? The presence of the first product should create a reversible connection between addition of the first and second substrate and should yield an intersecting initial velocity pattern. One possibility is that on formation of the Schiff base and release of water an associated conformational change excludes water from the active site making this step irreversible. Although perhaps possible, this seems unlikely in view of the observation that the intermediate is accessible to $NaBH_4$ since the intermediate can be reduced with this reagent (Shedlarski & Gilvarg, 1970; Laber et al., 1992). In contrast to the ping pong kinetic mechanism seen at high pH, at low pH the initial velocity pattern is of the intersecting type which indicates a sequential kinetic mechanism. The dead-end inhibition patterns obtained at low pH differ from those observed at high pH and are consistent with a steady state ordered kinetic mechanism with pyruvate binding to enzyme prior to ASA (Scheme 2). The change from a ping pong mechanism to a sequential one at low pH suggests that the Schiff base intermediate is readily hydrolyzed at low pH making the first half-reaction reversible. Shedlarski and Gilvarg (1970) proposed a chemical mechanism for DHDPS which involves proton abstraction at the methyl carbon of pyruvate in Schiff base with an enzymic lysine residue to form an enamine

Scheme 2

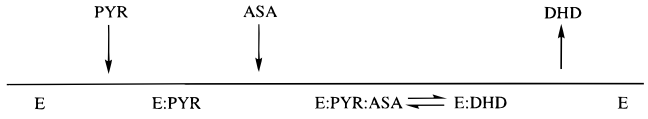

intermediate. Formation of the enamine intermediate and loss of the abstracted proton to solvent in all probability constitutes the irreversible step along the reaction pathway required of the ping pong kinetic mechanism observed at high pH since reprotonation of this system would be required to reverse the first half-reaction. If the p*K* for the system is significantly lower than the pH at which these studies were performed than the equilibrium would lie in favor of enamine formation, the enamine would form and basically await binding of ASA. If true, at lower pH values, at or below the p*K* for the enamine intermediate, the kinetic mechanism would be expected to be sequential as observed. In addition, it has been shown that the enzyme, when incubated with tritiated pyruvate, will catalyze the loss of tritium in the absence of ASA (Shedlarski & Gilvarg, 1970) suggesting that the enamine does form in the absence of ASA. It is therefore likely that a shift in the equilibrium in favor of the enamine at high pH, making loss of the proton effectively irreversible, leads to the ping pong kinetic mechanism seen at high pH. The data supports the original suggestion for the involvement of an enamine intermediate in the chemical mechanism (Shedlarski & Gilvarg, 1970).

The series of pyruvate analogs examined can provide information concerning the pyruvate binding site geometry of DHDPS. β-Fluoropyruvate binds to enzyme with a K_i value similar to $K_{pyruvate}$. Glyoxalate, an analog smaller than pyruvate, has a K_i value more than one order of magnitude lower than the 2-keto analogs. The enzyme is less tolerant to increases in analog size. 2-ketobutyrate binds with a K_i value that is about 4-fold greater than $K_{i,\beta\text{-fluoropyruvate}}$, suggesting that an increase in size results in weaker binding probably due to steric interference. However, a further increase in size has little additional effect, as evidenced by 2-ketovalerate with a K_i value that is very similar to the K_i value for 2-ketobutyrate. The similarity between the K_i for succinic semialdehyde and K_{ASA} suggests that the amino group of ASA plays little or no role in the binding of ASA to enzyme. This conclusion must be tempered by the fact that K_m values for substrates are often not equal to substrate dissociation constants.

Mechanism of Allosteric Inhibition. The cooperative inhibition displayed by L-lysine and AEC and the asymptotic approach of activity to a finite value as the inhibitor concentration approaches saturation are indicative of only partial inhibition at saturating levels of inhibitor, consistent with these compounds being allosteric inhibitors as suggested previously. At high pH the uncompetitive inhibition patterns of AEC and L-lysine vs pyruvate suggest that the inhibitor may bind to the F enzyme form, downstream from the form to which pyruvate binds. L-Lysine has been reported to be a competitive inhibitor vs ASA for the wheat (Kumpaisal et al., 1987) and *E. coli* enzymes (Yugari & Gilvarg, 1962). However as shown in these studies, the L-lysine inhibition pattern vs ASA displays an intercept effect which shows that, at saturating levels, ASA does not eliminate the inhibition by L-lysine, indicating that if L-lysine binds to the ASA binding site, as proposed by Kumpaisal et al. (1989), it does not bind to that site alone. The apparent L-lysine $I_{0.5}$ values would be expected to increase with increasing ASA concentrations if ASA and L-lysine compete for the same site, but this is not observed since the $I_{0.5}$ value is the same regardless of substrate concentrations. The inhibition patterns and the observation of partial inhibition by L-lysine instead suggest that L-lysine binds to a site different than the active site, but on the same enzyme form (F) as ASA binds and diverts reaction flux to an alternative slower pathway.

Scheme 3

$$E + A \underset{k_2}{\overset{k_1}{\rightleftharpoons}} E{:}A \underset{k_4}{\overset{k_3}{\rightleftharpoons}} F{:}H^+ \xrightarrow{k_5} F + H^+$$

$$F + B \underset{k_8}{\overset{k_7}{\rightleftharpoons}} F{:}B \underset{k_{10}}{\overset{k_9}{\rightleftharpoons}} E{:}Q \xrightarrow{k_{11}} E + Q$$

In order to further investigate the mechanism of L-lysine inhibition at high pH, initial velocity patterns were obtained in the presence of different concentrations of L-lysine. Theory describing the use of initial velocity patterns obtained in the presence of an allosteric effector to determine the mechanism of inhibition or activation is described in Cook (1982) and Payne et al. (1991). Briefly, the technique involves treating the allosteric effector, in this case L-lysine, as a pseudo-reactant and observing how each kinetic parameter is influenced by the presence of the effector. Which parameters are affected, and to what degree, is determined by examination of secondary replots of the initial velocity patterns performed at zero and increasing effector concentrations. When the kinetic mechanism is known, the enzyme forms the effector binds to may be identified from the enzyme distribution equations. For the DHDPS ping pong mechanism $V/K_{pyruvate}$ represents E and V/K_{ASA} represents F. As indicated in Table 3 the values of $V/K_{pyruvate}$ are unchanged in the presence of L-lysine while the values of V/K_{ASA} and V are reduced by a maximum of about 90% of the value in the absence of L-lysine as determined from the secondary replots of the data. The results indicate that L-lysine must bind to F and does not cause, at saturating concentrations, complete inhibition of the DHDPS reaction. Figure 3 and the data in Table 3 indicate that lysine is not a competitive inhibitor vs ASA for the enzyme from *E. coli* and also indicates that L-lysine does not compete with ASA for F in a mutually exclusive fashion, but rather diverts reaction flow to an alternative slower pathway. Furthermore, the results suggest that the second half reaction is rate limiting for the overall reaction since V and V/K_{ASA} are similarily affected. AEC displays a behavior qualitatively identical to that of L-lysine, although AEC binds to DHDPS with lower affinity and provides less inhibition at saturating levels. An overall kinetic mechanism that takes into account allosteric L-lysine inhibition at high pH is presented in Scheme 1. The mechanism of release of DHD and L-lysine cannot be obtained from the present data and is reflected in the dashed arrows shown in Scheme 1.

As indicated by the effects of L-lysine on V/K_{ASA}, lysine must bind to F and must slow down a step or steps in the second half-reaction. In a ping pong mechanism, V/K_{ASA} begins with free F and ends with the first irreversible step which is release of DHD. A slow release of L-lysine subsequent to release of DHD or a slow enzyme conformational change following L-lysine release regenerating free E can be ruled out since these effects would be present only on V and not on V/K_{ASA}. The equation that describes the ping pong kinetic mechanism of the DHDPS reaction at high pH is shown in Scheme 3 where A is pyruvate, B is ASA, H^+ is a proton, and Q is DHD. The kinetic equations for

Scheme 4

$$E + A \underset{k_2}{\overset{k_1}{\rightleftharpoons}} E{:}A \underset{k_4}{\overset{k_3(B)}{\rightleftharpoons}} E{:}A{:}B \underset{k_6}{\overset{k_5}{\rightleftharpoons}} E{:}P \xrightarrow{k_7} E + P$$

this mechanism are as follows:

$$V/K_{\text{pyruvate}} = k_1k_3k_5(A)/(k_2k_4 + k_2k_5 + k_3k_5) \quad (7)$$

$$V/K_{\text{ASA}} = k_7k_9k_{11}(B)/(k_8k_{10} + k_8k_{11} + k_9k_{11}) \quad (8)$$

$$V = k_3k_5k_9k_{11}(E_t)/(k_4 + k_5 + k_{10} + k_{11}) \quad (9)$$

Since the effects of L-lysine inhibition are manifested on V/K_{ASA} and V, the microscopic rate constants that L-lysine effects must be contained in the equations for both V/K_{ASA} and V. The shared rate constants are k_9, k_{10}, and k_{11}. The rate constant k_{11} represents product release, while the constants k_9 and k_{10} are not simple microscopic rate constants but, in the mechanism of Scheme 3, represent the chemical portion of the second half-reaction and may include enzyme conformational changes. L-Lysine must slow down one or more of these steps. Since the specific step(s) lysine effects cannot be determined from the present data, additional studies will be required to elucidate the exact nature of lysine inhibition.

At low pH L-lysine also inhibits the DHDPS reaction, but the values of the L-lysine dissociation constants are about 1 order of magnitude greater than they are at high pH. There are no L-lysine pK values in the range of pH values tested, so the decrease in affinity cannot be accounted for by protonation of an L-lysine functional group. A second possibility for the change in affinity could be due to protonation of an enzymatic group involved in L-lysine binding at the lysine binding site and cannot be ruled out. A third possibility that may account for the lower affinity at low pH, is that the enzyme form that L-lysine has the most affinity for at high pH, namely the enzyme−enamine intermediate, is largely absent at low pH as suggested by the change in kinetic mechanism.

The equation for the steady state ordered mechanism the DHDPS reaction conforms to at low pH is shown in Scheme 4 where A is pyruvate, B is ASA, and P is DHD. The kinetic equations for this mechanism are as follows:

$$V/K_{\text{pyruvate}} = k_1(A) \quad (10)$$

$$V/K_{\text{ASA}} = k_3k_5k_7(B)/(k_4k_6 + k_4k_7 + k_5k_7) \quad (11)$$

$$V = k_5k_7(E_t)/(k_6 + k_7) \quad (12)$$

In the mechanism of Scheme 4, V/K_{pyruvate} represents free enzyme. There is an approximately 10-fold decrease in V/K_{pyruvate} with increasing pyruvate concentrations and indicates that L-lysine can bind to free enzyme, but with a dissociation constant 10-fold greater than for binding to the F enzyme form at high pH. For a typical steady state ordered mechanism k_1 would represent the rate constant for formation of the complex between enzyme and first substrate. In the case of DHDPS, k_1 is likely a macroscopic rate constant, and may contain microscopic rate constants associated with the chemical steps involved in the formation of the enzyme Schiff base (these steps occur in the absence of ASA at high pH). One or more of these rate constants are affected by bound lysine to result in the 10-fold decrease in V/K_{pyruvate}. At low pH the rate constants k_5, k_6, and k_7 are equivalent to the rate constants k_9, k_{10}, and k_{11} represented in Scheme 3

Scheme 5

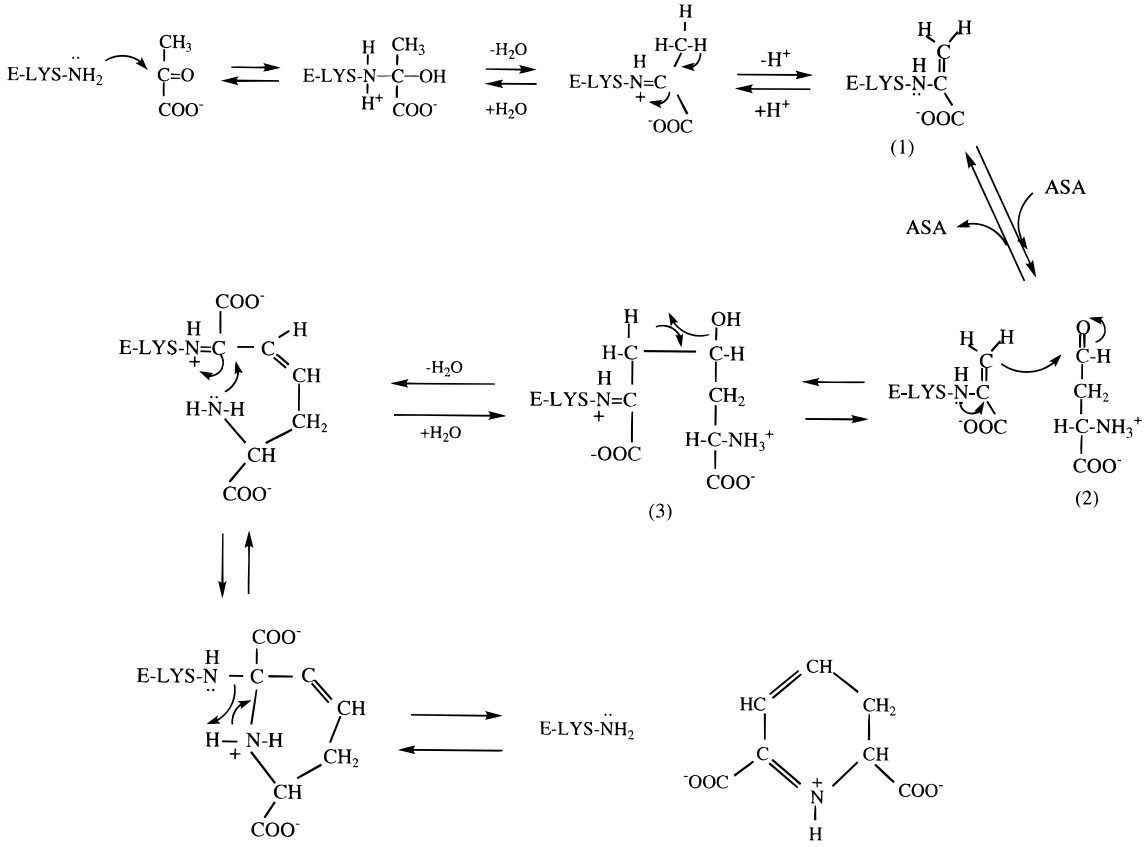

for the reaction at high pH. At low pH k_5, k_6, and k_7 are the shared rate constants in the equations for V/K_{ASA} and V and one or more of these are slowed down by bound L-lysine by a factor of about 10 as also seen at high pH.

Chemical Mechanism of DHDPS. The data are consistent with the chemical mechanism proposed for DHDPS illustrated in Scheme 5. After pyruvate binds to enzyme, the uncharged ϵ-amino group of an active site lysine residue (Lys161) attacks the carbonyl carbon of pyruvate, and, with subsequent elimination of water leads to formation of a Schiff base intermediate. Loss of a proton from the β-methyl of the pyruvyl−Schiff base intermediate, likely assisted by an active site general base, forms an enamine intermediate indicated by "(1)". The enzyme−enamine is the F enzyme form if the general base loses its proton to solvent. Following ASA binding, an aldol condensation reaction initiated by attack of the enamine intermediate on the carbonyl carbon of bound ASA will lead to structure "(3)". Deprotonation of the α-amine of ASA and transimination results in closure of the ring to form product, DHD, followed by expulsion of the lysine residue. Assuming ASA binds to enzyme with the α-amine protonated, this would require deprotonation of the amine functional group in "(2)" to initiate the transimination reaction. The various enzymatic groups present to assist in the catalytic steps are not shown in Scheme 5. The proposed mechanism is similar to the earlier one proposed by Shedlarski and Gilvarg (1970). These authors suggested the possibility that after ASA binds to enzyme the transimination reaction might occur prior to the aldol condensation forming a Schiff base intermediate that could close the ring to form DHD by an intramolecular aldol condensation. However, these authors also showed that the enzyme, in the absence of ASA, could catalyze the loss of tritium from tritiated pyruvate. This observation and the kinetic data presented here argue for the sequence of steps illustrated in Scheme 5.

ACKNOWLEDGMENT

The author wishes to thank Dr. Ronald E. Viola and Dr. Lakshmi Cyr for supplying the ASA used in these studies and Dr. Paul F. Cook for a critical reading of the manuscript and support to initiate these studies.

REFERENCES

Bonnassie, S.; Oreglia, J., & Sicard, A. N. (1990) *Nucleic Acids Res. 18(N21)*, 6421.

Borthwick, E. B., Connell, S. J., Tudor, D. W., Robins, D. J., Shneier, A., Abell, C., & Coggins, J. R. (1995) *Biochem. J. 305*, 521−524.

Bouvier, J., Richaud, C., Richaud, F., Patte, J.-C., & Stragier, P. (1984) *J. Biol. Chem. 259*, 14829−14834.

Black, S., & Wright, N. G. (1955) *J. Biol. Chem. 213*, 39−50.

Cheshire, R. M., & Miflin, B. J. (1975) *Phytochemistry 14*, 695−698.

Cleland, W. W. (1977) *Adv. Enzymol. 45*, 273−387.

Cleland, W. W. (1979) *Methods Enzymol. 63*, 103−138.

Cook, P. F. (1982) *Biochemistry 21*, 113−116.

Dereppe, C., Bold, G., Ghisalba, O., Ebert, E., & Schar, H.-P. (1992) *Plant Physiol. 98*, 813−821.

Dixon, M., & Webb, E. C. (1979) in *Enzymes*, 3rd ed., Academic Press, New York.

Farkas, W. & Gilvarg, C. (1965) *J. Biol. Chem. 240*, 4717−4722.

Frisch, D. A., Gengenbach, B. G., Tommey, A. M., Sellner, J. M., Somers, D. A., & Myers, D. E. (1991) *Plant Physiol. 96*, 444−452.

Halling, S. M., & Stahley, D. P. (1976) *Biochim. Biophys. Acta 452*, 580−596.

Karsten, W. E., & Viola, R. E. (1992) *Biochim. Biophys. Acta 1077*, 209−219.

Kumpaisal, R., Hashimoto, T., & Yamada, Y. (1987) *Plant Physiol. 85*, 145−151.

Laber, B., Gomis-Ruth, F.-X., Romao, M. J., & Huber, R. (1992) *Biochem. J. 288*, 691−695.

Mazelis, M., Whatley, F. R., & Whatley, J. (1977) *FEBS Lett. 84*, 236−240.

Mirwaldt, C., Korndorfer, I., & Huber, R. (1995) *J. Mol. Biol. 246*, 227−239.

Payne, M. A., Rao, G. S. J., Harris, B. G., & Cook, P. F. (1991) *J. Biol. Chem. 266*, 8891−8896.

Richaud, F., Richaud, C., Ratet, P., & Patte, J.-C. (1986) *J. Bacteriol. 166*, 297−300.

Sambrook, J., Fritsch, E. F., & Maniatis, T. (1989) in *Molecular Cloning*, Cold Spring Harbor Laboratory Press, Plainview, NY.

Segel, I. H. (1975) in *Enzyme Kinetics*, John Wiley & Sons, New York.

Shames, L., & Wedler, F. C. (1984) *Arch. Biochem. Biophys. 235*, 359−370.

Shedlarski, J. G., & Gilvarg, C. (1970) *J. Biol. Chem. 245*, 1362−1373.

Stahley, D. P. (1969) *Biochim. Biophys. Acta 191*, 439−451.

Wallsgrove, R. M., & Mazelis, M. (1981) *Phytochemistry 20*, 2651−2655.

Yamakura, F., Ikeda, Y., Kimura, K., & Sasakawa, T. (1974) *J. Biochem. 76*, 611−621.

Yugari, Y., & Gilvarg, C. (1962) *Biochim. Biophys. Acta 62*, 612−614.

Yugari, Y., & Gilvarg, C. (1965) *J. Biol. Chem. 240*, 4710−471.

BI962264X